DFT Investigation of Bi (100) and Au (111) for Heavy Metal Ion Adsorption and Selective Comparison for Water Quality Sensing Electrodes

Arivarasi A

Department of Electrical & Electronics Engineering,
Bits Pilani Dubai Campus, Dubai, UAE
P20140002@dubai.bits-pilani.ac.in

Anand Kumar

Department of Electrical & Electronics Engineering,
Bits Pilani Dubai Campus, Dubai UAE.
akumar@dubai.bits-pilani.ac.in

***Abstract* - Bismuth Film Electrodes are promising environment-friendly sensors, replacing toxic mercury to detect heavy metal ions. Experimental studies report diverse selectivity responses for Pb, Cd, and Zn through voltammetry, which requires a nominal selectivity estimation mechanism to experiment ionic responses for 3D printed Bismuth electrode. Density functional theory and simulation are used for experimental verification. Nanoporous gold surface possesses high surface to volume ratio providing better selectivity for multiple ion detection in aqueous media. To scientifically understand the adsorption mechanism and to compare electrode characteristics we carry out Discrete Fourier Transform, DFT, calculations on chemical interactions between heavy metal ions and Bi, Au surfaces at an atomistic level. A similar study exists in literature, for selective identification of Pb (II) by DFT calculation, through which chemical interactions between exfoliated ZrP and heavy metal ions were carried out. Through the current DFT study for Bismuth and Gold, simulation results indicate comparative statistics through detailed metallic analysis. The selectivity of Bi surface (through DFT Simulation) towards Pb, Cd and Zn ions shows a response in the range of Pb > Cd > Zn. Similarly gold surface shows relative higher selective figures in the order of Zn > Cu > Fe > Cr > T i > Ni > Pb. As a result, NPGF shows more metallic character than Bismuth. While Bismuth electrode is suited for Pb^{2+} detection, Porous Gold electrode would be a choice for ions like Cu^{2+}, Zn^{2+}, and Cr^{3+} which are verified through simulation results.**

Keywords - DFT simulation, Bismuth, adsorbance, selectivity, electrochemical sensing

I. INTRODUCTION

Electrochemical sensors can be miniaturized; they are environmentally friendly, economical and easy to use. Therefore, these sensors are widely used in environmental monitoring systems [1]. For over a decade, Bismuth electrode responses have been measured through electrochemical experiments [2] through electrochemical experiments; these experiments are possible since Bi (100) exhibits metallic surface behavior. Weitzel and Micklitz [3, 4] reported superconductivity in Bismuth granular films. While surfaces play a key role in superconductivity, the Bi (100) surface has several surface related Fermi-level crossings that is similar to the behavior of Bi (111) surface. Bi (100) is found to exhibit better metallic surface, due to the presence of electronic surface states, restricting accuracy to finite thickness [5]. Experimental research has demonstrated the functionality of electrodes modified with Bismuth precursor compounds. A Bismuth-based disposable sensor has been developed by Rosalina et al. [6] for Hydrogen Sulfide gas detection. For water quality sensors, Bismuth electrodes, with lower toxicity, have replaced Mercury electrodes [1]. Serrano et al. reported that Bismuth can be deployed in water sources [7]. Carbon electrodes were modified with Bismuth oxide nano-particle through a sparking process, applying a high voltage. Lee et al. measured the effect of Zn, Cd and Pb concentration on a nano-Bi electrode of 100 nm width. The Square Wave Anodic Stripping Voltammetry (SWASV) curve showed peaks which are due to the oxidation of Zn, Cd, and Pb: the intensity of peak current increases with increasing concentrations [23] of these ions. Recently it is claimed that screen-printed electrodes simplify processing. The ink is synthesized by one step sol-gel and pyrolysis [10] of Bismuth nano particles and amorphous Carbon. As a result, the sensitivity to Zn (II) is not affected by stripping mixture while the sensitivity to Cd (II) and Pb (II) decreases. When Bismuth coated electrodes provide high precision when used in electrochemical sensing [15]; these experimental results indicate higher sensitivity towards Zinc [11]. The relative importance of surface is higher for smaller sensor structures; with screen printing, the incorporation of Bismuth is a challenging step in in-situ production, ex-citu production [7], drop casting method [12], and sparking method [13]. These tests and stripping experimental techniques are carried out in acidic medium. However, there are *diverse figures of selective ranges* when it comes to detection of heavy metal ions using bismuth electrode. Different researchers have reported different ranges and limit of detection for sensitivity and selectivity of Bismuth electrode [7, 10, 14, 15]. For water quality sensing, the consistency in selectivity of Bismuth films towards different heavy metal ions is of interest.

A. Related Work

A modeling and simulation-based method would provide a means to evaluate and validate experimental results.

Density Functional Theory (DFT) functionals [8] have been used to analyze surface behavior by correlating energy, charge, current, and potential through electrostatics. DFT studies can be used to determine the selectivity of an electrode towards metal ions; such studies were carried to determine the selectivity and sensitivity of ZrP towards Pb (II) ions. With the combined experimental and theoretical efforts, a new route to realizing improved selectivity in electrochemical sensing of toxic metal ions was formulated and demonstrated. While Wang et al. [16] performed effective combined experimental and DFT study to determine the selectivity of ZrP towards lead ion, DFT verification studies (with heavy metal ion) have not been carried out for bismuth modified electrodes; experimental results are available for sensitivity and selectivity of bismuth modified electrodes. Moreover, to substantiate, DFT study of CO_2 adsorption of Bi_2MoO_6 surface has been carried out [54] for interaction study.

Practically, electrochemical applications involve nanoporous gold or bismuth surfaces for detecting heavy metal ions. Nanoporous gold contains small sized pores in nanometer sizes, employing a highly selective process. As a result, gold nanoparticles are used for environmental analysis. Also, it possesses high electrical conductivity and surface to volume ratio.

Application of gold surfaces is of potential research interest [18]. Wei et al. [19] studied free energy computation on Au (111) surface and its electron transfer efficiency. There exists strong binding between Au (111) and peptide aromatic groups. Several kinds of protein adsorptions were experimented [20, 21, 22] with Gold surfaces. While protein adsorption is widely studied, ionic interactions on the Gold surface are rarely performed through DFT mechanism. Adsorption of atomic oxygen on Au (321) surface was studied through an effective and comparative DFT investigation [17, 45]. Also, adsorption of cysteine on flat and chiral gold surfaces was investigated. Eventually, the highly selective electrode for particular ions could be identified. Hence modeling of sensor selectivity response through DFT investigation for Gold is important. By comparing the DFT study, a better electrode is identified for usage by selective comparison of ion selectivity through simulation. Electrodes are selected for usage mainly based on quick ionic response and number of detectable ions. Au (111) surface is shown to be more suitable [9] as the experimental scenarios require isothermal conditions. Au (111) orientation provides infinite, perfect, atomically closed packed face-centered cubic (fcc) surface [24]. Subsequently, both metallic surfaces are investigated through DFT mechanism for comparison.

B. DFT

DFT is a computational modeling mechanism using molecular structures to calculate optimized energies in material science. Through the behavior of electrons in interacted surfaces, before and after effects are quantitatively studied. Here the electrode properties are analyzed based on surface charge transfer phenomenon and band gap, determining conductive nature along with other metallic properties [17] [31] [36].

In this paper, the adsorption and selectivity of Lead, Cadmium, Zinc ions on Bismuth surface and Zinc, Copper, Iron, Lead, Chromium, Nickel, Titanium interactions on Gold surface are studied, simulated, analyzed and compared through DFT study. Huang et al. [25] experimented for ionic interactions on the Gold surface. 3D printable Bismuth and Gold electrodes require a reference selectivity value; the existing experimental results for the selectivity of such electrodes show a great deal of variability and hence do not provide an accurate means to determine this reference selectivity value. Hence computational tools are used to provide a reference ionic selectivity indication through energy calculations for Bismuth and Gold Surfaces. DFT study through computational analysis can characterize the selective nature of ion adsorption based on energetic values [26]. A similar study was performed in [16] for ZrP. The DFT study in this paper analyzes and compares the optimized and stable adsorption mechanism of Bismuth and Gold structure in the presence of selected ions. The study is new for Bismuth and Gold simulation and comparison. Such a unique DFT based study is useful for verification of electrochemical experimental responses. The organization is such that analysis of Gold follows Bismuth simulations in each section. Section II details computational details of Bi and Au molecular simulation using ADF and Gaussian tools respectively. Subsections detail their geometry structure. Section III details results and discusses the optimized strucutres and compares the populated surface charges. Band gap is analyzed in subsections and subsequently used for detailed electrode comparison in Section V. Simulation is compared with already experimented selectivity figures in Section IV. Section V discusses the electrode properties and tabulates a comparative table.

II. COMPUTATIONAL DETAILS

Calculations are performed on Crystallographic Input File (CIF) based on Bismuth unit cell. The basis set used is Triple Zeta with a Polarization (TZP) function under Slater Type Orbitals (STO) [4, 27, 28] and the processing parameters include atomic mass and nuclear charges. The Generalized Gradient Approximation (GGA) [29, 30] / Perdew-Bruke-Ernzerhof (PBE) [14] exchange correlation is used. A Bismuth super cell of size 2X2X1 is used in the simulations. A thick slab comprising of 24 Bismuth atoms (hexagonal structure) is constructed with a vacuum space to enable smooth relaxation. The vacuum region in lattice vectors ensures internal surfaces do not interact and periodicity of the supercell further necessitates this vacuum region. The choice of supercell structure enables accurate convergence. In the current study, Bismuth is modeled and

optimized for periodic structures using a single slab of 24 atoms.

Further, DFT study is performed on the 12 Gold atoms. Geometry is optimized using UB3LYP to obtain converged energy. The surface is designed using Gaussian 09 / Gauss View 5.0.9. The calculation method used is B3LYP using LANL2DZ basis set. The calculation method, basis set and input details are supplied to the tool for optimizing modeled structure as in Table I.

TABLE I. GOLD STRUCTURE AND COMPLEX OPTIMIZATION DETAILS

Au Orientation	111
Calculation	Au (UB3LYP)
Methods (In brackets)	Au with ions (RB3LYP) B3LYP / LANL2DZ
Basis set	LANL2DZ
Number of gold atoms	12
Number of ion	1
Type of charge population analysis	Mulliken

C. Geometry

All the atoms in super cell are relaxed and optimized for energy. The Bismuth layers are designed in CIF file structure. As per lattice parameters of the hexagonal Bi primitive cell, the length of real space lattice vectors are 17.14 Å, 17.14 Å and 94.49 Å respectively as in Fig. 1; in reciprocal k-space (Fourier Transform of the Bismuth real lattice structure), and the lattice vectors are 0.423 Å, 0.423 Å and 0.066 Å respectively. Fig. 2(a) describes the structure of Bismuth atoms after optimization. Fig. 2(b) describes Bismuth structure with Lead ion adsorbed on the top surface. Fig. 2(c) and Fig. 2(d), respectively, are the Bismuth structure with adsorbed Cadmium and Zinc ions. The smallest inter atomic distances are 3.1143 Å (Bi12 to Bi(15) for Bismuth with adsorbed Lead ion; 3.1143 Å (Bi20 to Bi24) for Bismuth with adsorbed Cadmium ion; and 3.1655 Å (Bi12 to Bi16) for Bismuth with adsorbed Zinc ion (the inter atomic distances are marked with black arrows in figures 2(b), 2(c) and 2(d) respectively). Lead, Cadmium and Zinc atoms have real space lattice vectors of 9.99 Å and reciprocal k-space lattice vectors of 0.1756 Å. The lattice pair angle remains at 120º, 90º, 90º for Bismuth with adsorption. The convergence criteria are set in Amsterdam Density Functional (ADF). ADF is a DFT program particularly strong in understanding and predicting structure, reactivity, and spectra of molecules. DFT Calculations are performed using the ADF computational chemistry program. Optimization is done using periodic DFT code of ADF/BAND program (atomic-orbital based DFT program for periodic systems). It employs density functional theory in the Kohn-Sham approach. All atoms of Bismuth are completely relaxed and optimized before ionic elements gets adsorbed on (100) surface.

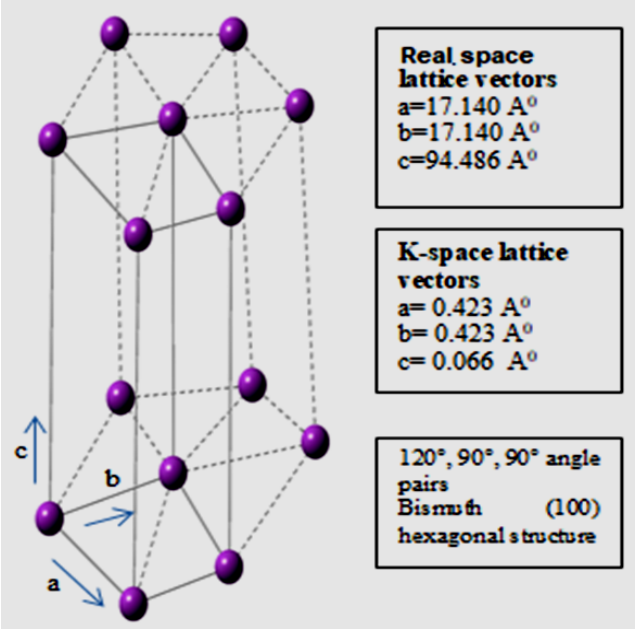

Figure 1. Hexagonal Bismuth Structure

The geometry of gold structure before and after optimization is provided. Thereby the distance in angstroms between each atom is set. Inter atomic distance is higher in positioning Gold atoms considering the high surface area to increase conductivity. Visualization of single layer optimized Gold (111) surface is presented in Fig. 3(a) and 3(b). Subsequently, the positions of 12 Au atoms after convergence are provided. Reported adsorption energies out of convergence are analyzed. The structures of optimized gold with ionic interactions are shown in Fig. 4. Individual ions are made to interact on the surface of Gold. Figure 4(a) to 4(g) shows the visualization of Gold surface interacted with ions such as Zn, Cu, Fe, Pb, Cr, Ni, Ti. The graph showing adsorption energies through DFT study is provided in Fig. 5(a). Magnitude of Zn shows higher value followed by Cu and Fe. Trend of adsorption energy in keV is provided in Fig. 5(b), which reflects the interaction study results through individual convergence run results.

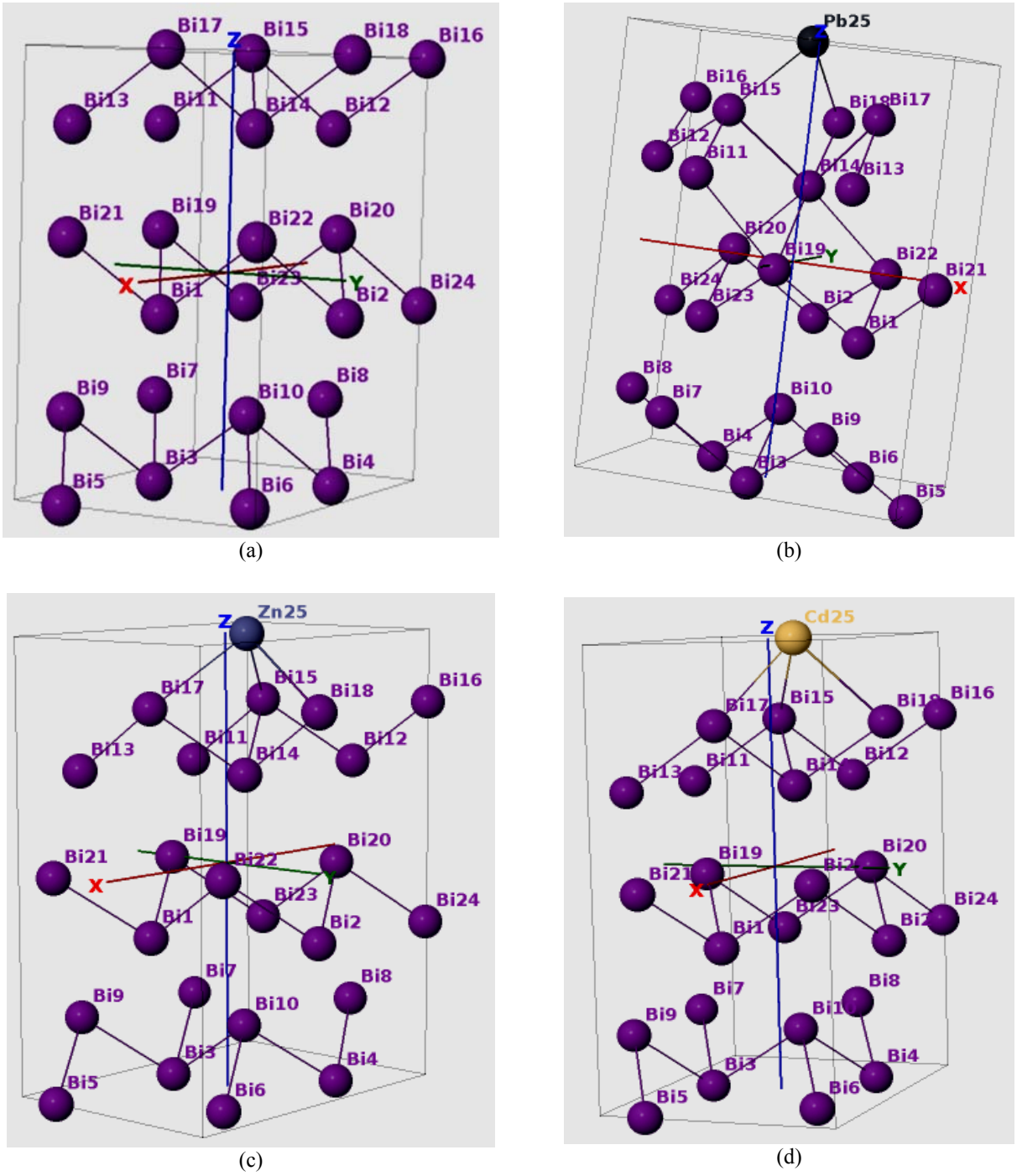

Figure 2. Optimized geometries with slabs and vacuums defined inside a box structure to visualize the ionic adsorption of Lead, Cadmium and Zinc on the top of Bismuth atomic structure. (a) Bismuth structure without ions in balls and sticks format (b) Bismuth with Lead ion interaction (c) Bismuth with Cadmium ion interaction in wireframe format (d) Bismuth with Zinc ion interaction for 2x2x1 supercell, after convergence of complete cell structure, containing 24 atoms. Units are in Å for lattice vectors.

All the atoms in the provided structure is relaxed and optimized before adsorption of ions. Gaussian program finds the closest minimum using the minimum descent with steps proportional to negative gradient. The optimization is performed for individual ionic interactions and results recorded. The heavy metal atoms such as Cu, Cr, Fe, Ni, Pb,

Ti, and Zn are adsorbed on with gold surface and optimized. Optimization includes placement of atoms in periodic spaces and providing input parameters for DFT calculation.

The program that terminates normally is analyzed for minimized adsorption energy, charge distribution and band gap. Tab. III lists converged energy data. Binding energy is the energy needed to completely remove an electron from the atom. Binding energy or ionization potential pattern for specific ions is analyzed.

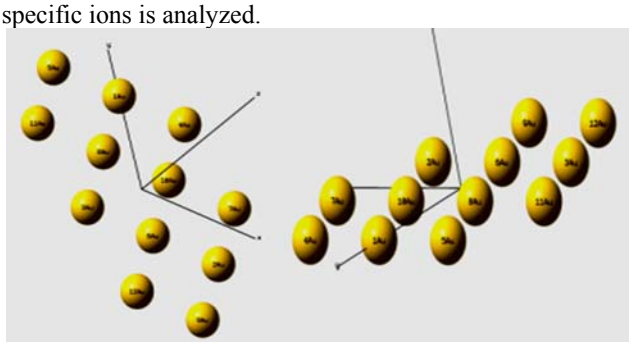

-a -b

Figure 3. Optimized gold structure having 12 Au atoms in a periodic structure. (a) Optimized gold structure: Visualization 1 (b) Optimized gold structure: Visualization 2.

III. RESULTS AND DISCUSSION

The results obtained are adsorption energies, surface charges and band gap. Based on the results, analysis is performed for before and after ionic interaction mechanism. Mullikan population analysis is followed for surface charge population on sensor surface. Band gap is directly obtained in ADF tool, whereas in Gaussian band gap is calculated using HOMO-LUMO energy differences, which are plotted in graphs. The discussion routes to the electrode property analysis.

D. Adsorption Energies

The energy calculations for converged atomic structure adsorption energies are tabulated in Tab. II calculated using Eq. (1), (2), (3) and (4) for individual ions. Eq. (1) is the generic formula. Eq. (2) is used for Lead ion interaction calculation; Eq. (3) for Cadmium ion and Eq. (4) for Zinc ion based calculations. Fig. 5 plots the optimized chemisorption energies, based on Table II.

Chemisorption energies are calculated [32] as:

$$E_{ads} = E_{hmi+bismuth} - (E_{bismuth} + E_{hmi}) \quad (1)$$

For Lead ion on Bismuth

$$E_{ads} = E_{bi+pb} - E_{bi} + E_{pb} \quad (2)$$

For Cadmium ion on Bismuth:

$$E_{ads} = E_{bi+cd} - E_{bi} + E_{cd} \quad (3)$$

For Zinc ion on Bismuth:

$$E_{ads} = E_{bi+Zn} - E_{bi} + E_{Zn} \quad (4)$$

The net adsorption energy E_{ads} is the difference of total energy of converged atomic structure of Bismuth and adsorbed ion (Pb, Cd or Zn), represented as $E_{hmi+bismuth}$. The sum of energies of converged structure of individual heavy metal ion (Pb, Cd or Zn), are represented as E_hmi and the converged energy of bismuth to be $E_{bismuth}$. $E_{hmi+bismuth}$ is the energy calculated for lead adsorbed on Bismuth surface, Cadmium adsorbed on Bismuth surface or Zinc adsorbed on bismuth surface depending on whether Lead, Cadmium or Zinc is adsorbed. The notation 'hmi' denotes heavy metal ion.

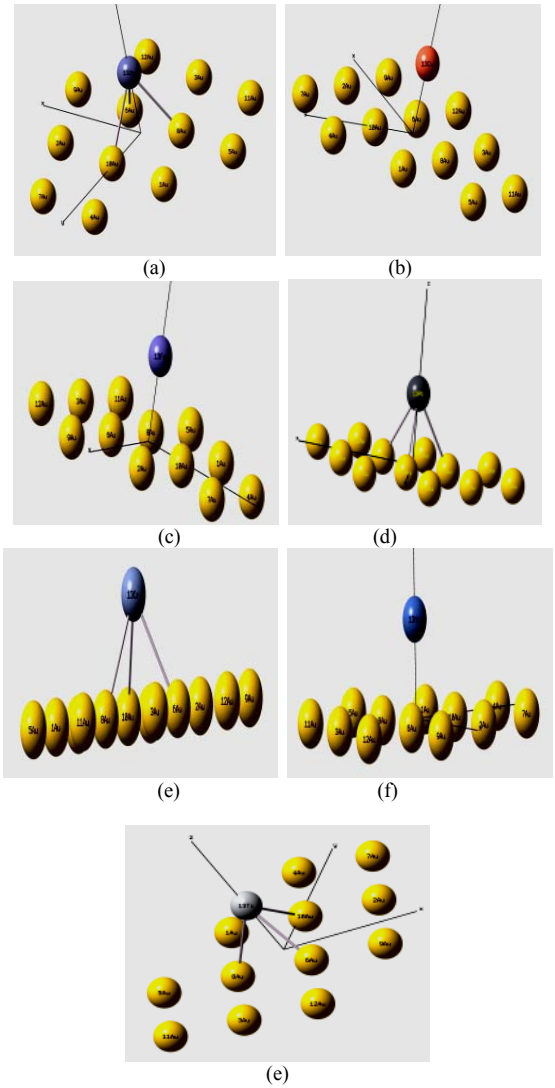

(a) (b) (c) (d) (e) (f) (e)

Figure 4. Structures of Au surface with Zn, Cu, Fe, Pb, Cr, Ni, Ti ionic interactions (a) Ionic interaction of Au with Zn (b) Ionic interaction of Au with Cu (c) Ionic interaction of Au with Fe (d) Ionic interaction of Au with Pb (e) Ionic interaction of Au with Cr (f) Ionic interaction of Au with Ni (g) Ionic interaction of Au with Ti

When binding energy is the energy of chemical bond between adsorbed molecule and particular atom on surface, the absorbed energy is based on inter ionic interactions. If physisorption, binding energy depends on the polarizability and number of atoms. Chemisorption refers to stronger perturbation of electronic structure of corresponding molecule. The energies will be in electron volts range. The adsorption leads to relaxation of the adsorption site, where the direction of relaxation is outwards from the metal surface [34].

Chemisorption energies are used to understand molecule interactions and metal surfaces, ordered structures, adsorbate interactions and to examine defects, bonding energies etc., [3]

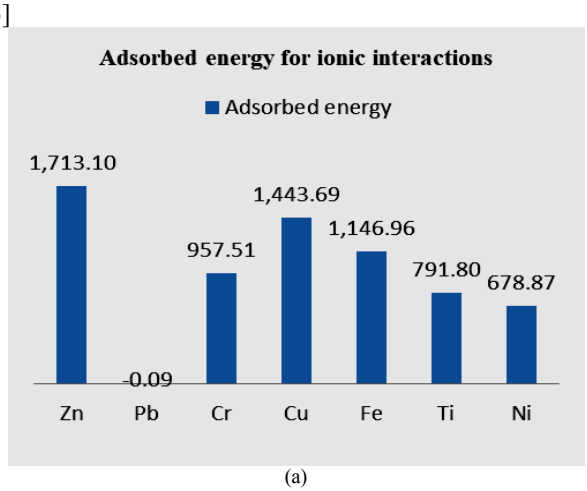

(a)

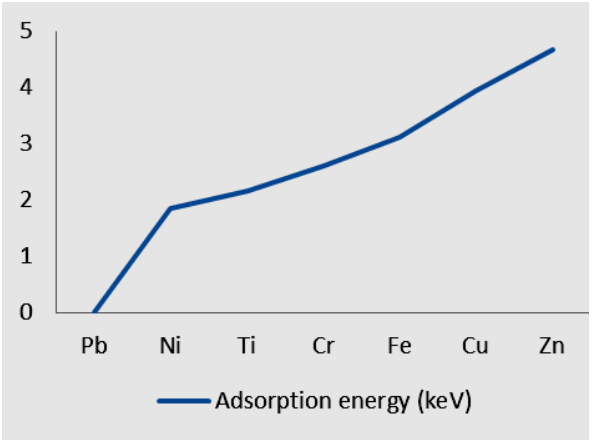

(b)

Figure 5. Adsorption energy plots Adsorbed energy of heavy metal ions on gold (b) Trend of adsorption energy converted to kilo electron volts.

The Optimized periodic structure of Bismuth super cell has converged planar structural modifications, resulting in kinetics of surface bonding [35]; adsorption, bonding and surface kinetics are correlated. Any molecule is stable if there are more attractive forces and reduced repulsive forces: attractive forces reduce the potential energy resulting in enhanced stability. This principle is used in optimization to determine most stable configuration with adsorption.

Optimized energy of Bismuth is provided in Column 1 of Table II. Column 2 refers to Bismuth with heavy metal ions' optimized energy. Column 3 refers to only ionic energy. Column 4 refers the specific ion for interaction. Column 5 indicates the net optimized energy value. Thereby, the converged atomic energies by optimization are provided in Table II.

TABLE II. CONVERGED ATOMIC STRUCTURE ENERGIES BASED ON ADSORPTION ENERGY CALCULATIONS (IN KCAL/MOL)

Only Bi E(Bismuth)	Bi with ion E(hmi +Bismuth)	Only ion E(hmi)	Ion for adsorption	Net Energy Value E_{ads}
-1968.80	-2019.88	0	Lead	-51.07
-1968.80	-1976.05	0	Cadmium	-7.24
-1968.80	-1975.28	0	Zinc	-6.46

In the case of chemisorption, electronic transfer between atoms takes place. The molecule may be torn apart, to satisfy valence requirements of surface metal atoms. As a result, a molecule can lose its identity during the surface interaction process. The stability order of metal ion adsorbed on Bismuth surface is: $Pb^{2+} > Cd^{2+} > Zn^{2+}$. Atomic structure with less potential energy is less stable. Lower stability of ion on Bismuth surface translates to lower adsorption, lower ionic selectivity and lower chemisorption of the ion on Bismuth surface. The adsorption sites of lead, cadmium and zinc atoms after energy based optimization are (-0.082, 0.956, 7.200) (0.350, 0.680, 7.4) and (0.310, 0.705, 7.155) respectively.

TABLE III. GOLD COMPLEX DFT CALCULATIONS

Au Converged Energy	**Converged Energy After Interaction**	**Ionic Energy**	**Adsorption Energy**
-1625.98	-1690.98	-1778.10 (Zn)	1713.10
-1625.98	-1628.72	-2.65 (Pb)	-0.08
-1625.98	-1710.60	-1042.12 (Cr)	957.50
-1625.98	-1821.49	-1639.21 (Cu)	1443.69
-1625.98	-1741.47	-1262.44 (Fe)	1146.95
-1625.98	-1681.68	-847.5022 (Ti)	791.80
-1625.98	-1794.61	-1506.99 (Ni)	678.86

The optimized energies are verified using varying k-point convergent points. K-space sampling is performed using meshes of different sizes. (3x3x1), (3x3x7), (5x5x3), (5x5x1), (7x7x1) were employed for the convergence calculations. Fig. 6 ensures the aptness of convergence by representing cut off energy value in (3x3x7) having -1968.0727 kJ/mol and continues to have consistent energies. This matches with Bismuth optimized energy in Tab. II.

Positions of Pb, Cd and Zn are varied for their ionic positions as in Fig. 7. The position of Pb atom at (-0.082,-0.956, 7.260), returned to its original converged position (-0.082,0.956,7.200) after re-optimization, with a change in 'z' direction position by 0.06 Å. Similarly the Cd atom at (1.350, 1.686, 7.425) converged back to (0.350, 0.680,

7.400), with a change in (x,y,z) being (1, 1.006, 0.025) Å. The co-ordinates of Zn atom changed to (0.210, 0.825, 7.255) is set back to its original converged form, with (0.310, 0.705, 7.155) as co-ordinates with a change of (0.1,-0.12,-0.1) Å.

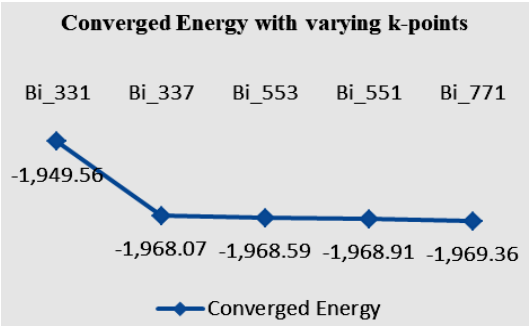

Figure 6. Optimized Bi (100) energies with varying k-points (y-axis is converged energies in electron volts

The stability of surface could be related with lowest surface free energy. Since the reference state in ADF is taken to be elemental ions, energy of individual Pb, Cd and Zn ions is optimized to zero. According to previous studies [36, 32], high negative adsorption energy obtained would lead to a more stable chemisorption. Moreover, out of electrostatic interaction, divalent cations have the lowest hydration energy and are preferably absorbed by cation exchangers [16].

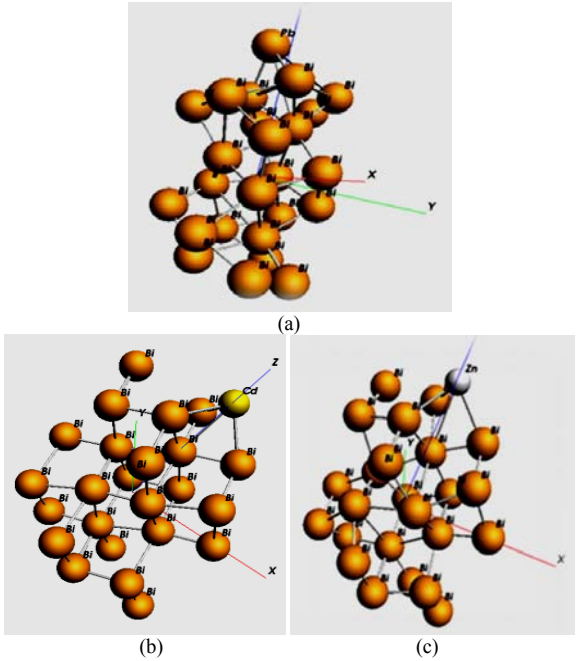

Figure 7. Optimization by changing atomic positions. (a) Position of lead (-0.08, -0.95, 7.26); (b) Position of cadmium (1.35, 1.68, 7.42); (c) Position of Zinc (0.21, 0.82, 7.25). After completion of optimization run, atoms return to their pre-optimized positions, confirming computational efficiency.

It is seen in Fig. 8 and Tab. II that Bismuth with adsorbed lead shows the highest stability. The Lead ion gets most selectively adsorbed towards defined Bismuth surface followed by Cadmium and Zinc. Hence, the DFT study indicates the ionic stability based on calculated minimum energy value. Also, the relative stabilities present on the atomic surface have the possibility to influence the individual stable energetic stabilities. Hence, the study mainly provides definitive conclusions on stability of adsorption towards Bi surface. The energy values depend on exchange correlation functional used. The study does not provide any conclusive inference on selectivity [26].

The crystal structure of Bi with solid solutions of Pb was experimented for surface resistance change [37, 34] lattice parameters, atomic parameters, temperature effects and compared for parametric changes; It reported no major changes in Pb with Bi, whereas surface changes were prominent for Sb with Bi (as an alloy). On the other hand, Bi (alloy) is proved for higher affinity with lead and lower ion flux persists with Zn and Cd [39].

Based on current DFT calculation using converged energies, the stability information is recorded. It also implies relative information among different ions that are simulated. Charge distribution and band gap information provides information on surface characteristics for Bismuth surface. Selectivty on ions depends on surface conductivity, wherein sensitivity of electrode and selectivity properties defines electrode characteristics in electrochemical sensor applications. The current simulation is of importance for heavy metal ion detection application based on bismuth.

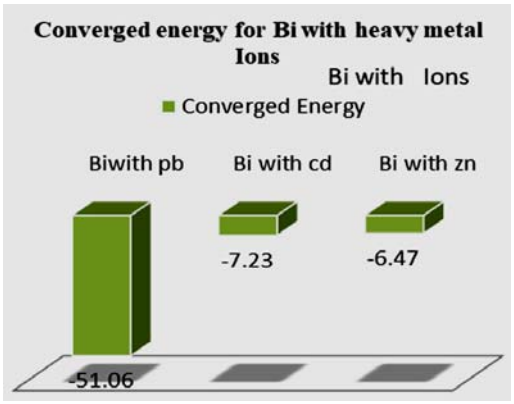

Figure 8. Converged energy for Bi with heavy metal Ions

Hereby, the Mulliken charge distribution and electronic structure [33] are analyzed for surface conductivity in subsequent subsection.

$$E_{ads} = E_{hmi+Au} - E_{Au} + E_{hmi} \quad (5)$$

The adsorption energy for study on Gold surface can be calculated using the Eq. (5). Net adsorption energy results from difference of energy obtained through ion interacted surface and individual sum of ion and surface energies. The energies are calculated through DFT mechanism and tabulated in Tab. III.

E. Mulliken Charge Distribution

Partial atomic charges are utilized to quantify the transfer of electrons between atoms in a material through computational calculations [30]. To observe chemical behavior through atomic charge concept, the net electronic and nuclear charge on each atom is preferred. Further, Mullikan charge is a result of Mullikan population analysis, which in turn is a result of partial atomic charge estimation. The method uses basis functions to represent molecular wave function. This charge based scheme assigns charge to atomic center, on the basis of the total electron density in basis functions. Eventually, charge per atom is derived from the weighted total of the product of density and overlap matrices [40, 41]. The method uses basis functions to define molecular wave functions. When an atom is expanded for its basis functions $X_u(r)$ having orbitals $\Psi(r)$, the density matrix D is defined by Eq. (6).

$$D_{(u,v)} = i_{occ}.\ n_i.\ C_{ui}\ .\ C_{vi} \tag{6}$$

where n_i = orbital occupations, i = orbital number, u and v are associated atom notations. C_{ui} and C_{vi} are linear coefficients.

Gross Mullikan population Q_u of basis function $\chi_{\mu(r)}$ is given in Eq. (7) where $D_{\mu.\mu}$ $S_{\mu.\mu}$ represents diagonal elements representing net mulliken population in molecule $v \neq u$.

$$Q_u = D_{u.u}\ Su.u + \Sigma\ 0.5(D_{u,v}\ S_{u,v} + D_{v,u}\ S_{v,u}) \tag{7}$$

Mulliken charge of atom A is calculated using the summation calculation of Q_u subtracted from atomic nuclear charge Z_A [41, 40] where $\mu\ \varepsilon\ A$ (Eq. 8).

$$Q_A\{\text{Mullikan}\} = Z_A - \Sigma\ Q_u \tag{8}$$

These calculations are utilized for Mullikan based charge model through ADF / BAND software.

While the population methods assign partial charge to atoms, Mullikan analysis is based on basis set which in turn apply partial charges [42]. The Mullikan charges are those, which are based on local electron density (or charge density), which depends on functional being used. The change in charge obtained by Mullikan population analysis is due to polarization and electron transfers [43]. Mullikan populations simplify the analysis on charge distributions [44]. On the basis of Mullikan charge analysis, the amount of charge variation for individual atoms can be tracked, which contributes to electrostatic potential [16]. It works by comparing changes in partial charge assignments between two different geometries when the same basis set is used [41]. The plot between individual bismuth atoms and Mullikan charges is provided in Fig. 9 for Lead, Cadmium and Zinc ion adsorptions. To compare before and after ion adsorption scenario, same functional and basis set is used. Mulliken charges vary through a magnitude due to the super-cell structure of 2X2X1.

The change in Mullikan charge after Lead ion adsorption is tracked using Fig. 10 and Tab. IV. For the surface bismuth atom, higher negative values (increase in charge) infers electrons being accepted to the surface. The charge transfer happens due to oxidation of Pb^{2+} cation. The Lead ion shows more positive charge as it loses electrons and charge transfer happens. After Bi (9), there is an indication of charge transfer after ion adsorption, which continues till Bi (25). Bi (9), Bi (10) possesses 0.1 unit changes in charge. Bi (12) to Bi (24) indicates electron transfer. Charge of lead ion is + 0.1993951 after adsorption occurs.

In Fig. 2, the Cadmium ion is adsorbed on bismuth surface. Mullikan charge distribution shows changes due to surface charge transfer of Cadmium ion on Bismuth surface. This charge transfer is due to losing or accepting electrons between surface and Cadmium ion. As the cations directly influence the surface charge carrier density and conductivity [31], the negative charges are increased on the bismuth surface thereby increasing the positive charge of Cadmium cation. Subsequent increase in surface charge of 0.1 units for Bi (15) through Bi (18) is recorded. Cd (25) shows + 0.1371487 charge units after adsorption. Comparing to lead ion adsorption, Cadmium ion changes shows nominal decrease in charge transfer analysis. Bi (17) through Bi (19) atoms undergo charge transfers and shows net change of 0.1 Mullikan charge units. Zn (25) shows lesser unit of charge transfer (+0.0542258) compared to Lead and Cadmium interaction. With respect to 25th atom in every case, nearly 0.2 unit change is seen for Pb atom interaction, 0.13 for Cd and 0.05 for Zn, indicating conductivity changes at atomic level.

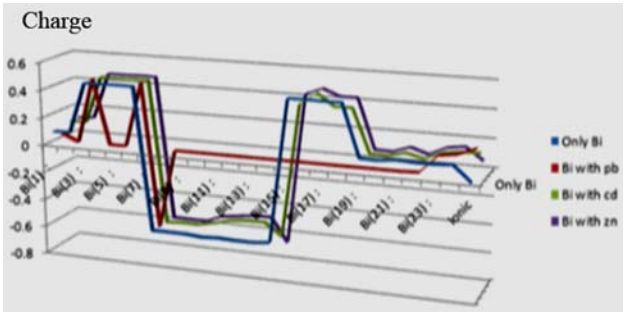

Figure 9. Charge population (unit in atomic units).

charge differences, the Mullikan population analysis implies higher charge transfer towards Lead ion on Bismuth structure compared to Cadmium and Zinc. As Zinc cation shows lesser charge transfer and lesser changes in surface charges, adsorption stability has reduced compared to previous cases. Cation retains a positive charge state after adsorption. The positive adsorption energy after optimization implies the lesser stability of Zinc cation towards Bismuth surface. As a result, the interaction which happened is not strong chemisorption. Comparing Bi surface, atoms from Bi (16) to Bi (24) has altered their

charges. Surface atoms Bi (15) through Bi (18) shows significant surface charge transfers, exhibiting ionic bondings, among which Lead interactions shows higher difference of +0.2901973 charge units. The surface charge transfer is higher for Lead atom and hence shows higher changes compared to Cadmium and Zinc as in Figure 10. Adsorption study based on energy characteristics implied greater changes for Lead only. Cadmium and Zinc showed equally lesser in magnitude, whereas charge based study shows Lead and Cadmium with nearly equal differences, with lesser changes in Zinc.

The charge differences for the Bismuth surface atoms which are Bi (9) to Bi (19) have undergone most of notable charge transfers with cations as in Tab. IV. The charge difference is higher for Lead following Cadmium and Zinc. The net Mullikan population charge differences with Bismuth atom are provided for comparison in Fig. 10.

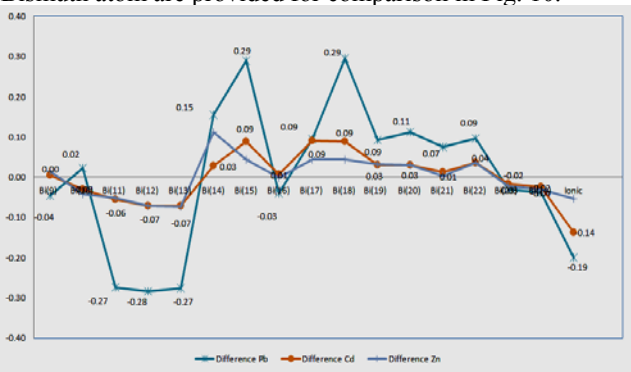

Figure 10. Plot of bismuth charge differences after ionic interactions selected for Bi (9) to Bi (24) atoms (unit in atomic units)

TABLE IV. CHANGE IN CHARGE WITH DIFFERENCE VALUES OF BISMUTH ATOMS AFTER IONIC INTERACTIONS

Bismuth atoms	Difference Pb	Difference Cd	Difference Zn
Bi(9)	-0.05	0.00	0.01
Bi(10)	0.02	-0.03	-0.04
Bi(11)	-0.27	-0.06	-0.05
Bi(12)	-0.28	-0.07	-0.07
Bi(13)	-0.28	-0.07	-0.07
Bi(14)	0.15	0.03	0.11
Bi(15)	0.29	0.09	0.04
Bi(16)	-0.04	0.01	0.00
Bi(17)	0.09	0.09	0.04
Bi(18)	0.30	0.09	0.04
Bi(19)	0.09	0.03	0.03
Bi(20)	0.11	0.03	0.03
Bi(21)	0.07	0.01	0.00
Bi(22)	0.10	0.04	0.04
Bi(23)	-0.03	-0.02	-0.02
Bi(24)	-0.04	-0.02	-0.03
Ion	-0.20	-0.14	-0.05

Negative overlap population indicates magnitude of comparable anti-bonding strength, and for the current case Lead shows more bonding compared to Cd and Zn.

In a molecule, the bonding overlaps relates to atomic interactions. The higher the charge transfer, greater the bonding capacity and surface conductivity. As the surface becomes more conductive on ionic contact, the response is sensitive to variations in specific parameters. The surface bonding is chemisorption, compared to physisorption for lead, which makes it more stable. Mullikan population hence provides a quantitative output of difference between numbers of electrons on the isolated free atom to the gross atom population, through the evident charge transfers on bismuth surface. The relative magnitude (change) phenomenon can be correlated for selective adsorption of experimental techniques for heavy metal ions, considering energy, charge variations.

Charge transfers of Gold surface are studied through Mulliken analysis. Total charge before and after optimization is different due to transfer of ionic charge. Sum of mulliken atomic charges changes after ionic interaction on surface. The charge population is provided for each atom through Gaussian tool. The sum of Mullikan charge for Au complex is higher compared to before interaction. Tab. V provides charge of Au surface before and after Zn ionic interaction. Other ions of study undergo a similar surface effect.

TABLE V. CHARGE OF AU SURFACE BEFORE AND AFTER ZN IONIC INTERACTION. (A.U) REFERES TO ATOMIC UNITS

Charge of Au	Charge of Zn ion	Charge after ionic Interactions (a.u)
0.04	2	0.16
0.047	2	0.16
0.047	2	0.16
-0.15	2	-0.00
-0.15	2	-0.00
0.25	2	0.24
-0.15	2	-0.00
0.25	2	0.24
-0.15	2	-0.00
0.25	2	0.24
-0.15	2	-0.009
-0.15	2	-0.09
		0.83
Sum of Mulliken Atomic charges =0		Sum of Mulliken Atomic charges = 2.0

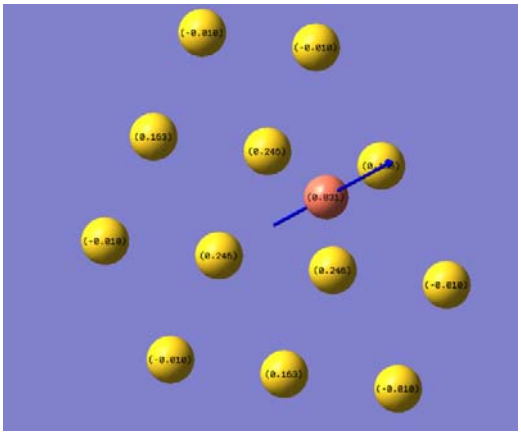

Figure 11. Au with Cu: Mulliken charge population

Charge distribution for ions is pictorially given for Cu and similar charge population happens for other ions on test. Fig. 11 picturizes Mullikan charge population of Cu ion interaction on gold surface. Sum of mulliken atomic charge before interaction is null. After the Cu ion is adsorbed on surface, sum of Mullikan atomic charge is two for the surface molecular structure. A positive charge of 0.831106 implies losing of electrons to Gold surface. Atom numbers three and five has increased electro negativity due to electron acceptances. Similar charge sharing of ions with Gold surface is observed for all simulated ions.

F. Band Structure and DOS

The band structure of bismuth is studied from earlier times [46, 47, 48]. Analysis and study results of the band structure calculation for bismuth were compared with experimental data [47].

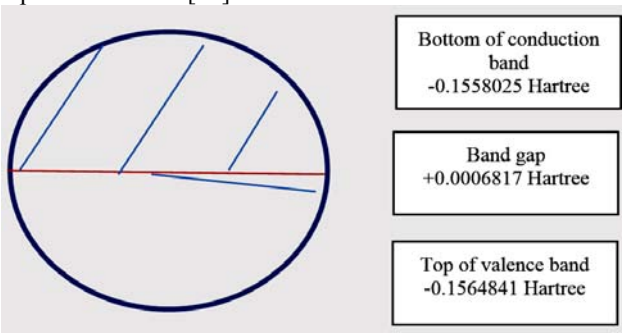

Figure 12. Band gap of bismuth.

The authors have measured the effective masses for electrons and holes. The study explains the electronic states in the vicinity of fermi level through augmented plane wave method at points gamma, T, L and X of the brillouin zone. Analysis reveals about de Haas-van Alphen period of Bismuth alloy through electronic study [38]. Normally, the uppermost valence band has high mobility and low effective mass, whereas lower valence band has lower mobility and high effective mass [49]. Effective mass determines energy at different states that make band displacements in T, L based on symmetry [47]. Period of oscillation of the effect is inversely proportional to area of cross section of fermi distribution in momentum space and it can vary with number of electrons. This effect can be correlated with donors and acceptor potentials on bismuth surface. The number of free electrons and holes in bismuth as per referred study is $1.5X10^{-5}$ [48]. The bonding nature is analyzed with respect to valence charge density transfer [55] exposing different natures of the bond for bismuth III-V compounds like BBi, AlBi, GaBi and InBi.

The band gap for bismuth as per the band diagram from BAND system is 0.0185 eV (+0.00068 hartree) as in Fig. 12, where Bi(100) possesses less symmetry than Bi (111). Differences between Bi (100) and Bi (111) in the inter layer relaxation and minor angstrom variations in displacements would affect negligibly on surface adsorption energy phenomena. The displacements are found to be less than 0.1 Å [5], whereas experimental band gap is 0.3 eV corresponding to absorption minimum [55]. The number of valence electrons for the structure is 5, having $6s^2p^3$, wherein indirect band gap is measured to be 0.086 eV. For semi-metals, which have a very narrow band gap, there are superimpositions of unoccupied energy orbitals from valence to conduction-bands. Fermi level region has unoccupied p-orbital region superimposed on conduction band. The band diagram shows direct band gap as the valence and conduction bands lie on the same k-point axis. There are more fermi level crossings, where the s-orbitals are placed in valence band only.

By electronic band structure studied by Golin et al. [48], the structure is in agreement with optical data and effective mass anisotropies. The spin orbit coupling terms in perturbation theory are of consideration. Specific surface spin states are described for Bi, paving way for spintronics and valleytronics. It can be inferred that, Bi surface can be exploited for its surface state properties [49]. Only the valence band and lower part of conduction bands are of importance for analysis. Lead has $6s^2p^2$ valence configuration (upon losing of electrons), whereas Bismuth has $6s^2p^5$ valence configuration (upon gaining). Fig. 14 shows filled in p and s orbitals, electrons partially occupying conduction band. DOS is higher compared to Bismuth condition in conduction band. Similarly, Cadmium electronic interchange happens with Bismuth followed by orbital changes. Here the DOS is comparatively lesser. The valence $4d^{10}$ shares electrons with $5s^2$ of Bismuth. $3d^{10}$ of Zinc is represented through the density of states and lesser amount of conduction states exists comparatively. When $4s^2$ electrons have been transferred to bismuth, it possess $6s^2p^5$ valence, after gaining of electron. Movement of electrons from valence to conduction band contributes to electric current and in this case it is ionic current. The comparative analysis graph on Bismuth, Bismuth with Lead, Bismuth with Cadmium, and Bismuth with Zinc interactions

in atomic level is shown in Fig. 13. Bismuth with Cadmium and Zinc shows similar conduction behavior when compared with Bismuth combined with Lead cation at atomic level. Fermi level crossings with respect to k-points shows significant movement of electrons from valence to conduction band with charge contributions. Band gap is zero after ionic interaction inferring metallic nature.

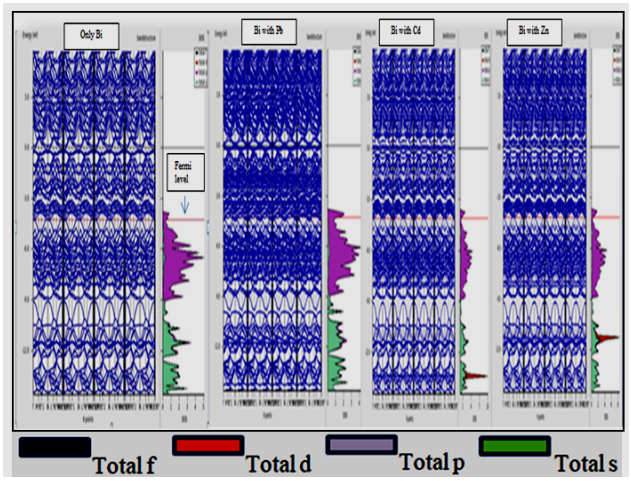

Figure 13. DOS comparative levels

As the Density Of States (DOS) is measured using the above plots, density of states of Bismuth in conduction band lies at 0.8 eV^{-1} per unit energy. DOS is measured as number of states per unit energy per unit volume [50]. The Fermi level is shown in red colour. The density of states in valence band lies below fermi level graphically, whereas above red line lies conduction band energy states. The conduction band of Bismuth with Lead ion is at 2.2 eV^{-1} per unit energy, which is higher, compared to Cadmium and Zinc values. DOS of Bismuth with Cadmium ion is marked at 1.8 eV^{-1} per unit energy and DOS of Bismuth with Zinc ion marked at 1.5 eV^{-1} per unit energy as in Fig. 14(a) - 14(d).

Further, the band gap in optimized gold optimizated complex is analyzed. HOMO energy levels represents highest occupied molecular orbital and LUMO represents lowest unoccupied molecular orbital. The HOMO-LUMO ($E_{\_LUMO} - E_{\_HOMO}$) gap represents band gap, which is very less for metals as provided in Tab. VI. These frontier orbitals are represented through 3D orbital diagrams in gaussian tool. Fig. 15(a) and Fig. 15(b) presents optimized Gold particles Au (111) plane, single layer with Cu^{2+} LUMO and HOMO representations. Ionization energy depends on the negative value of HOMO energy represented in Tab. VI.

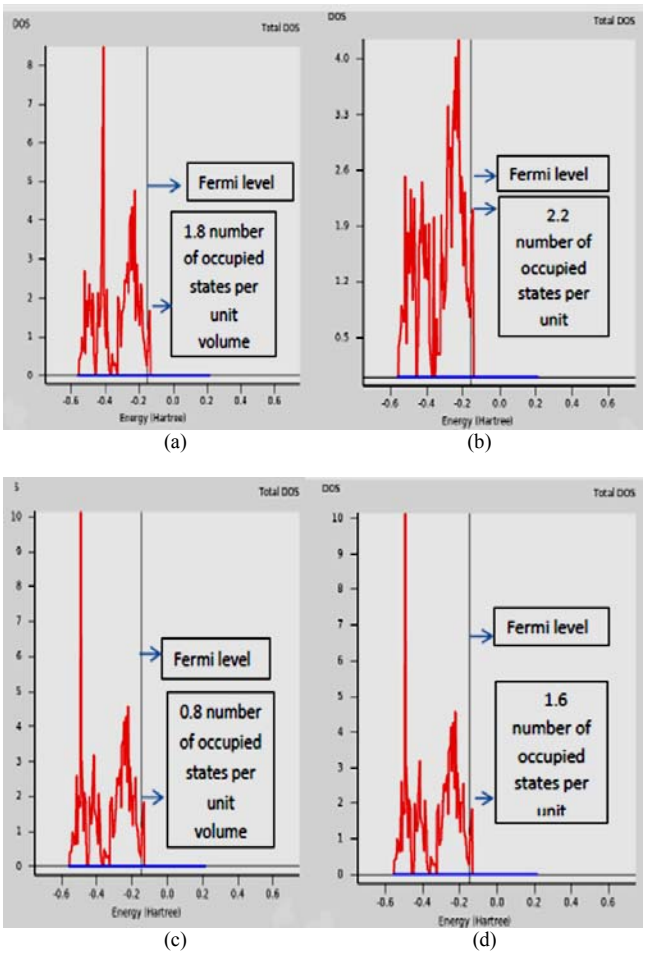

Figure 14. DOS comparative levels with respect to energy (a) DOS only for bismuth (b) DOS for Pb ion bonded on Bi (c) DOS for Cd ion bonded on Bi (d) DOS for Zn ion bonded on Bi

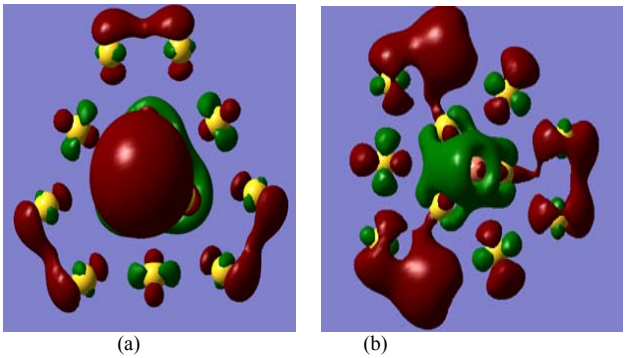

Figure 15. HOMO and LUMO picturization of Orbitals in Gaussian tool (a) HOMO molecular orbital representation (b) LUMO molecular orbital representation.

TABLE VI. BAND GAP AND IONIZATION ENERGY

Compound	HOMO [Ha]	LUMO [Ha]	$E_{LUMO} - E_{HOMO}$	$-E_{HOMO}$ Ionization energy
Zn^{2+}	-0.46	-0.40	0.06	0.46
Cr^{2+}	-0.46	-0.40	0.06	0.46
Cu^{2+}	-0.36	-0.35	0.00	0.36
Fe^{2+}	-0.38	-0.36	0.02	0.38
Ni^{2+}	-0.36	-0.35	0.00	0.36
Pb^{2+}	-0.50	-0.50	0	0.50
Ti^{2+}	-0.46	-0.46	$-1e^{-05}$	0.46
Au only	-0.22	-0.16	0.05	0.22

Also, the table presents details on band gap and ionization energy values. When the amount of energy required to remove the loosely bound electron is lesser, the bond formation becomes a less complex reaction. Ionization energy is less for Zinc and Copper compared to lead interaction as in Fig. 16. Copper and Nickel shows the lower value of 0.36013. Lead has a band gap of zero which is purely metallic.

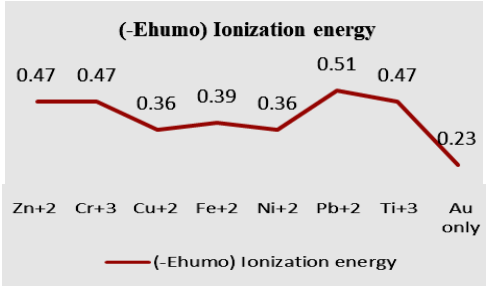

Figure 16. Plot of Ionization energy (Ionization energy Vs. ions of interest)

IV. EXPERIMENTAL SELECTIVITY BASED ON BISMUTH AND GOLD

Lee et al. [55] introduced bismuth nanopowders based electrochemical sensor using screen printed electrode fixed with nafion on a carbon electrode. The quantitative analysis for sensitivity and selectivity were proved for Pb, Cd and Zn ions. In another scenario, Granadorico et al. designed and tested a disposable electrochemical sensor [51]. The sensor was tested for selected heavy metal ions Pb(II), Cd(II) and Zn(II) co-deposited with Bismuth on Carbon screen printed electrode. The square wave anodic stripping voltammetry provided detection limits in $ngml^{-1}$ in 120s. This is a potential environmental heavy metal sensing mechanism.

Similarly, Vlastimil et al. performed square wave voltammetry for heavy metal ion detection using Bismuth Film Electrode (BiFE), instead of mercury based electrode. Detection limits was found to be $2.9X10^{-9}$ mol/L for Pb(II), $2.4X10^{-9}$ mol/L for Cd(II) and $1.2X10^{8}$ mol/L for Zn(II). Zinc has lesser sensitivity and selectivity towards bismuth.

Armstrong et al. investigated Bi based electrodes for three metal ions (lead, cadmium and zinc) in the range of 10-100 gL^{-1} range with a detection limit of 105, 54 and 396 ngL^{-1}. The square wave stripping voltammograms obtained using BiFE in 0.1 mol/L acetate buffer (pH=4) at different concentrations of metal in a pre-concentration time of 120s is recorded. Normally, the electrode is polarized to a suitable cathode potential, and the metal precursor is reduced to the respective metal, forming a thin film [52]. Subsequently, performance of BiFE for determination of Pb(II), Cd(II) and Zn(II) on various Carbon substrates was demonstrated by Wang. et al [12].

TABLE VII. SENSITIVITY REFERENCES

Heavy metal Cations	Sensitivity	Reference
Cu^{2+}	<1 pM	Gooding et al. (2009)
Divalent heavy metal ions	Nm	Kim et al. (2001)
Cu^{2+}	$58.76\mu A\mu M^{-1}$	Huang et al. (2009)
Hg^{2+}	1Pm	Zhang (2014)

Further, Gooding et al. [53] developed a sensor for detecting Cu ions with detection limit below 1 pM. Gold nano particles provide quick response and increased sensitivity in aqueous media. Hence it is used to create highly sensitive electrodes. Environmental sensing using Gold nano particle electrodes is prevalent in detection of chemical pollutants in water. Tab. VII is based on Gold electrode response to detect heavy metal ions. Therein, the simulation study goes in line with already reported experimental studies. Also, responses of potential electrodes can be verified using DFT study for selectivity before any such experimentation.

V. ELECTRODE PROPERTY BASED ON DFT STUDY

The adsorption energies in keV and eV representing normalized Gold and Bismuth single surface values are presented in Fig. 17(a) and Fig. 17(b). Nanoporous Gold Film (NPGF) electrode surface shows more metallic character than Bismuth electrode. Adsorption is purely a surface phenomenon and consequence of surface energy. Due to the metallic bonding characteristics of Gold constituent surface atoms, the simulated DFT model resulted in higher adsorption energy. This is a good indicator to be used as sensing electrode.

When the calculated DFT energies are positive, it is an exothermic reaction. Negative DFT energies indicate endothermic reaction. All ions except Pb adsorbed on gold electrode undergo exothermic reaction. Bismuth based responses are endothermic. For an endothermic reaction, electron affinity is negative and energy is absorbed as heat. For an exothermic reaction, electron affinity is positive. Energy is usually released as heat, but can also be in electric form or light or sound. The energy needed for the reaction to occur is less than the total energy released.

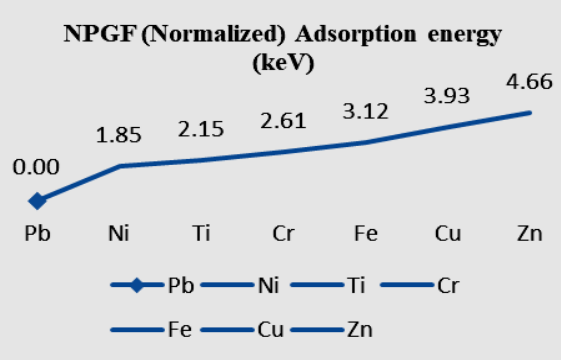

(a)

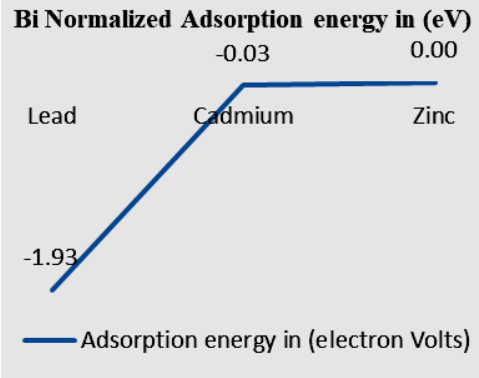

(b)

Figure 17. Gold and Bi plots in KeV and eV unit ranges.

The normalized NPGF adsorption energy trend implies higher binding energy on Au surface. Bi electrode provides normalized adsorption energy in eV as per the plots. Electrodes that exhibit higher surface energies are more stable for ionic adsorption. Among the different types of bonding, metal surface to metal atoms possess metallic type of bonding. This is applicable only to chemisorption. Apart from Pb (Au surface), Zn and Cd (Bi surface), all other ions possess metallic bonding.

Summary and comparative analyses of simulated electrode characteristics are provided in Table VIII. While the electron affinity increases from left to right in periodic table (Au placed before Bi), the metallic behavior is stronger for Au surface.

The ionization energy increases from low to high from bottom to top of periodic table. Lead requires lower ionization potential than other ions. Electron sharing of Lead is higher compared to other ionic elements. Electron affinity follows the same sequence as ionization energy. Electron affinity depends on electrode surface and its sensitivity towards particular ions. Electron affinity can be measured by the amount of energy released when an electron is added to an atom to form a negative ion. Also, electrons based on metal are delocalized. Since the energy is in keV and positive, NPGF shows more metallic character than bismuth electrode. While Bismuth electrode is best suited for Lead detection, Porous Gold electrode would be best choice for ions like Cu^{2+}, $Zn2^{+}$ and Cr^{3+}.

TABLE VIII. ELECTRODE PROPERTIES BASED ON SIMULATION RESULTS

Ion	Electrode		Adsorption energy	Unit	Ionization Energy	Band Gap	Property	Sorption	Type of bond
	Gold	Bismuth							
Pb	x		-0.002429285	keV	0.50979		◊	ϕ	
		x	-2.2144753	eV	0†	0	◊	‡	√
Cd		x	-0.31376973	eV	0	0	◊	ϕ	
Zn	x		46.61596915	keV	0.468†	-0.06	Δ	‡	√
		x	-0.28032732	eV	0	0	◊	ϕ	
Cu			39.28494452	keV	0.36013†	-0.02	Δ	‡	√
Cr			26.05506336	keV	0.46759	-0.0605	Δ	‡	√
Fe			31.21028707	keV	0.38692	-0.024	Δ	‡	√
Ni			18.47293579	keV	0.36013	-0.026	Δ	‡	√
Ti			21.54600785	keV	0.46759	-0.062	Δ	‡	√
						x	Specific electrode		
						Relative absolute			
						†	Less Ionization energy		
						ϕ	Physisorption		
						‡	Chemisorption		
						√	Metallic		
						Δ	Exhibits exothermic property		

VI. CONCLUSION

The periodic DFT study for inferring selectivity, is carried out for Bismuth with ions of interest. The energetic and electronic properties were investigated. This is in line with DFT studies performed for exfoliated nano zirconium phosphate for lead ion detection, which was experimentally proved. But for bismuth, which needed computational DFT study, with experimental data being available, the selective adsorption is studied for specific and selective heavy metal ions. While the proposed methodology is to first perform DFT study using simulation prior to experimentation, where direct experimentation would be complex and providing inconsistent results without simulation comparison. Consistency in final results is ensured by the proposed approach. It is proved through performed simulations.

Adsorption of Lead ion shows more adsorbance towards Bismuth surface, followed by Cadmium and Zinc. Charge analysis shows considerable changes in Lead and Cadmium ion surface adsorption. Band gap of Bismuth is zero after ion adsorption, where in density of states changes. The result serves as base to compare the Bismuth electrode and its characterization towards ion adsorptions of Gold electrode through simulations. Band diagrams and DOS confirm changes in conductivity before and after ion adsorption. Charge transfer happens for Bi on contact with Pb/Cd/Zn ions. Hence modeling and simulation confirms the heavy metal ion adsorption on Bismuth electrode surface, which coincides clearly with experimental reports. Finally, the selectivity of Bi surface towards Pb, Cd and Zn ions, shows response in range of Pb>Cd>Zn. Similarly Gold surface show relative higher selective figures in the order of Zn^{2+}>Cu^{2+}>Fe^{2+}>Cr^{3+}>Ti^{2+}>Ni^{2+}>Pb^{2+}. NPGF shows more metallic character than Bismuth. While Bismuth electrode is suited for Pb^{2+} detection, Porous Gold electrode would be a choice for ions like Cu^{2+}, Zn^{2+} and Cr^{3+}. The results are verified through existing literature references on electrochemical experimentations.

Limitations about the simulation include compatible parametric comparison where the same tool could not be utilized for different metal surfaces. The result does not vary as same theoretical concepts are applied using different tools. If same tool could be used, the complexity of research is less and leads to increased compatibility in parametric analysis. Further the computational methodology can be applied for varied sensing metal surfaces. However band gap study can be further explored to have accurate analysis on conductive electrode surface nature.

ACKNOWLEDGEMENTS

Authors would like to thank BITS Pilani Dubai Campus for the computing facility. This work was done as part of Arivarasi's PhD research at BITS Pilani, Dubai Campus. Sincere acknowledgements to Dr. Eldhos Iype, Assistant Professor, Department of Chemical Engineering.

REFERENCES

[1] M. Granado Rico, M. Olivares-Marín and E. Gil, "A Novel Cell Design for the Improved Stripping Voltammetric Detection of Zn(II), Cd(II), and Pb(II) on Commercial Screen-Printed Strips by Bismuth Codeposition in Stirred Solutions", Electroanalysis, vol. 20, no. 24, pp. 2608-2613, 2008.

[2] G.Mills and G. Fones, "A review ofin situmethods and sensors for monitoring the marine environment", Sensor Review, vol. 32, no. 1, pp. 17-28, 2012.

[3] B. Weitzel and H. Micklitz, "Superconductiviy in granular systems built from well-defined rhombohedral Bi-clusters: Evidence for Bi-surface superconductivity", Physical Review Letters, vol. 66, no. 3, pp. 385-388, 1991.

[4] E. Van Lenthe and E. Baerends, "Optimized Slater-type basis sets for the elements 1-118", Journal of Computational Chemistry, vol. 24, no. 9, pp. 1142-1156, 2003.

[5] P. Hofmann, J. Gayone, G. Bihlmayer, Y. Koroteev and E. Chulkov, "Electronic structure and Fermi surface of Bi(100)", Physical Review B, vol. 71, no. 19, 2005.

[6] S.Rosolina, T. Carpenter and Z. Xue, "Bismuth-Based, Disposable Sensor for the Detection of Hydrogen Sulfide Gas", Analytical Chemistry, vol. 88, no. 3, pp. 1553-1558, 2016.

[7] N. Serrano, J. Díaz-Cruz, C. Ariño and M. Esteban, "Stripping analysis of heavy metals in tap water using the bismuth film electrode", Analytical and Bioanalytical Chemistry, vol. 396, no. 3, pp. 1365-1369, 2009.

[8] Z. ZOU, A. JANG, E. MACKNIGHT, P. WU, J. DO, P. BISHOP and C. AHN, "Environmentally friendly disposable sensors with microfabricated on-chip planar bismuth electrode for in situ heavy metal ions measurement", Sensors and Actuators B: Chemical, vol. 134, no. 1, pp. 18-24, 2008.

[9] J. Fajín, J. Gomes and M. Cordeiro, "DFT Study of the Adsorption of d-(l-)Cysteine on Flat and Chiral Stepped Gold Surfaces", Langmuir, vol. 29, no. 28, pp. 8856-8864, 2013.

[10] K. Armstrong, C. Tatum, R. Dansby-Sparks, J. Chambers and Z. Xue, "Individual and simultaneous determination of lead, cadmium, and zinc by anodic stripping voltammetry at a bismuth bulk electrode", Talanta, vol. 82, no. 2, pp. 675-680, 2010.

[11] J. Wang, J. Lu, S. Hocevar, P. Farias and B. Ogorevc, "Bismuth-Coated Carbon Electrodes for Anodic Stripping Voltammetry", Analytical Chemistry, vol. 72, no. 14, pp. 3218-3222, 2000.

[12] J.Wang, "Stripping Analysis at Bismuth Electrodes: A Review", Electroanalysis, vol. 17, no. 15-16, pp. 1341-1346, 2005.

[13] D. Riman, A. Avgeropoulos, J. Hrbac and M. Prodromidis, "Sparked-bismuth oxide screen-printed electrodes for the determination of riboflavin in the sub-nanomolar range in non-deoxygenated solutions", Electrochimica Acta, vol. 165, pp. 410-415, 2015.

[14] Y. Wang, T. Gould, J. Dobson, H. Zhang, H. Yang, X. Yao and H. Zhao, "Density functional theory analysis of structural and electronic properties of orthorhombic perovskite CH3NH3PbI3", Phys. Chem. Chem. Phys., vol. 16, no. 4, pp. 1424-1429, 2014.

[15] C. Mayorga-Martinez, M. Cadevall, M. Guix, J. Ros and A. Merkoçi, "Bismuth nanoparticles for phenolic compounds biosensing application", Biosensors and Bioelectronics, vol. 40, no. 1, pp. 57-62, 2013.

[16] L. Wang, W. Xu, R. Yang, T. Zhou, D. Hou, X. Zheng, J. Liu and X. Huang, "Electrochemical and Density Functional Theory Investigation on High Selectivity and Sensitivity of Exfoliated Nano-Zirconium Phosphate toward Lead(II)", Analytical Chemistry, vol. 85, no. 8, pp. 3984-3990, 2013.

[17] Yakovkin, I. (2005). DFT study of oxygen adsorption on W(112) surface. Surface Science, 577(2-3), pp.229-235.

[18] M. Ford, C. Masens and M. Cortie, "The Application of Gold Surfaces And Particles in Nanotechnology", Surface Review and Letters, vol. 13, no. 0203, pp. 297-307, 2006.

[19] T. Wei, H. Ma and A. Nakano, "Decaheme Cytochrome MtrF Adsorption and Electron Transfer on Gold Surface", The Journal of Physical Chemistry Letters, vol. 7, no. 5, pp. 929-936, 2016.

[20] T. Wei, M. Carignano and I. Szleifer, "Lysozyme Adsorption on Polyethylene Surfaces: Why Are Long Simulations Needed?", Langmuir, vol. 27, no. 19, pp. 12074-12081, 2011.
[21] T. Wei, S. Kaewtathip and K. Shing, "Buffer Effect on Protein Adsorption at Liquid/Solid Interface", The Journal of Physical Chemistry C, vol. 113, no. 6, pp. 2053-2062, 2009.
[22] Wright, P. Rodger, S. Corni and T. Walsh, "GolP-CHARMM: First-Principles Based Force Fields for the Interaction of Proteins with Au(111) and Au(100)", Journal of Chemical Theory and Computation, vol. 9, no. 3, pp. 1616-1630, 2013.
[23] M. Amjadi, A. Pichitpajongkit, S. Lee, S. Ryu and I. Park, "Highly Stretchable and Sensitive Strain Sensor Based on Silver Nanowire–Elastomer Nanocomposite", ACS Nano, vol. 8, no. 5, pp. 5154-5163, 2014.
[24] F. Hanke and J. Björk, "Structure and local reactivity of the Au(111) surface reconstruction", Physical Review B, vol. 87, no. 23, 2013.
[25] Huang and B. Lin, "Application of a nanoporous gold electrode for the sensitive detection of copper via mercury-free anodic stripping voltammetry", The Analyst, vol. 134, no. 11, p. 2306, 2009.
[26] B. Rosen and V. Percec, "A density functional theory computational study of the role of ligand on the stability of CuI and CuII species associated with ATRP and SET-LRP", Journal of Polymer Science Part A: Polymer Chemistry, vol. 45, no. 21, pp. 4950-4964, 2007.
[27] D. Chong, E. Van Lenthe, S. Van Gisbergen and E. Baerends, "Even-tempered slater-type orbitals revisited: From hydrogen to krypton", Journal of Computational Chemistry, vol. 25, no. 8, pp. 1030-1036, 2004.
[28] E.Engel and S. Vosko, "Exact exchange-only potentials and the virial relation as microscopic criteria for generalized gradient approximations", Physical Review B, vol. 47, no. 20, pp. 13164-13174, 1993.
[29] J. Perdew, K. Burke and M. Ernzerhof, "Generalized Gradient Approximation Made Simple", Physical Review Letters, vol. 77, no. 18, pp. 3865-3868, 1996.
[30] F. Jensen, Introduction to computational chemistry, 2017.
[31] F. Tian, L. Zhao, X. Xue, Y. Shen, X. Jia, S. Chen and Z. Wang, "DFT study of CO sensing mechanism on hexagonal WO3 (001) surface: The role of oxygen vacancy", Applied Surface Science, vol. 311, pp. 362-368, 2014.
[32] D. Changqing, "A Density Functional Investigation on C Atom Adsorbed on Ni (111) Surface in the Steam Reforming of Acetic Acid", in Power and Energy Engineering Conference (APPEEC), 2010 Asia-Pacific, 2010, pp. 1--4.
[33] D. HS, O. mw, K. Bs, P. SD, L. Hw and W. DM, "Thermoelectrics, 2007. ICT 2007. 26th International Conference on", in First-principles calculations on electronic structure of Pb{T}e, 2018, pp. 90--93.
[34] Y.Shevtsov and N. Beizel', "Pb distribution in multistep bismuth refining products", Inorganic Materials, vol. 47, no. 2, pp. 139-142, 2011.
[35] Y. Qian, M. Bedzyk, P. Lyman, T. Lee, S. Tang and A. Freeman, "Structure and surface kinetics of bismuth adsorption on Si(001)", Physical Review B, vol. 54, no. 7, pp. 4424-4427, 1996.
[36] V. Arce, R. Gargarello, F. Ortega, V. Romañano, M. Mizrahi, J. Ramallo-López, C. Cobos, C. Airoldi, C. Bernardelli, E. Donati and D. Mártire, "EXAFS and DFT study of the cadmium and lead adsorption on modified silica nanoparticles", Spectrochimica Acta Part A: Molecular and Biomolecular Spectroscopy, vol. 151, pp. 156-163, 2015.
[37] P. Cucka and C. Barrett, "The crystal structure of Bi and of solid solutions of Pb, Sn, Sb and Te in Bi", Acta Crystallographica, vol. 15, no. 9, pp. 865-872, 1962.
[38] M.Ferhat and A. Zaoui, "Structural and electronic properties of III-V bismuth compounds", Physical Review B, vol. 73, no. 11, 2006.
[39] J. Macanás, D. Muraviev, M. Oleinikova and M. Muñoz, "Separation of Zinc and Bismuth by Facilitated Transport through Activated Composite Membranes", Solvent Extraction and Ion Exchange, vol. 24, no. 4, pp. 565-587, 2006.
[40] M. SEGALL, C. PICKARD, R. SHAH and M. PAYNE, "Population analysis in plane wave electronic structure calculations", Molecular Physics, vol. 89, no. 2, pp. 571-577, 1996.
[41] R. Mulliken, "Electronic Population Analysis on LCAO–MO Molecular Wave Functions. II. Overlap Populations, Bond Orders, and Covalent Bond Energies", The Journal of Chemical Physics, vol. 23, no. 10, pp. 1841-1846, 1955.
[42] C.Pisani, Hartree-Fock ab initio treatment of crystalline systems. Berlin: Springer, 1988.
[43] N. Sato, E. Okamoto, T. Suzuki and Y. Seki, "Energy Dependence of Sensitivity and Its Control by Electrode Design in a-Si:H/c-Si Heterojunction Gamma-Ray Detectors for Dosimeters", Japanese Journal of Applied Physics, vol. 31, no. 1, 5, pp. 1524-1529, 1992.
[44] Zaragoza, R. Santamaria and R. Salcedo, "The interaction of vanadyl porphyrin with the HY zeolite surface", Journal of Molecular Catalysis A: Chemical, vol. 307, no. 1-2, pp. 64-70, 2009.
[45] V. Golovanov, M. Maki-Jaskari and T. Rantala, "Semi-empirical and ab initio studies of low-temperature adsorption of oxygen and CO at [110] face of SnO/sub 2/", IEEE Sensors Journal, vol. 2, no. 5, pp. 416-421, 2002.
[46] S. Golin, "Band Structure of Bismuth: Pseudopotential Approach", Physical Review, vol. 166, no. 3, pp. 643-651, 1968.
[47] C. Gallo, B. Chandrasekhar and P. Sutter, "Transport Properties of Bismuth Single Crystals", Journal of Applied Physics, vol. 34, no. 1, pp. 144-152, 1963.
[48] L. Ferreira, "Band structure calculation for bismuth: Comparison with experiment", Solid State Communications, vol. 5, no. 10, p. xix, 1967.
[49] H. Du, X. Sun, X. Liu, X. Wu, J. Wang, M. Tian, A. Zhao, Y. Luo, J. Yang, B. Wang and J. Hou, "Surface Landau levels and spin states in bismuth (111) ultrathin films", Nature Communications, vol. 7, p. 10814, 2016.
[50] T.H., "D. Sutton, Electronic spectra of transition metal complexes", Journal of Molecular Structure, vol. 4, no. 1, p. 116, 1969.
[51] V. Ivaništšev, R. Nazmutdinov and E. Lust, "A comparative DFT study of the adsorption of H2O molecules at Bi, Hg, and Ga surfaces", Surface Science, vol. 609, pp. 91-99, 2013.
[52] N. Lezi, C. Kokkinos, A. Economou and M. Prodromidis, "Voltammetric determination of trace Tl(I) at disposable screen-printed electrodes modified with bismuth precursor compounds", Sensors and Actuators B: Chemical, vol. 182, pp. 718-724, 2013.
[53] I. Goon, L. Lai, M. Lim, P. Munroe, J. Gooding and R. Amal, "Fabrication and Dispersion of Gold-Shell-Protected Magnetite Nanoparticles: Systematic Control Using Polyethyleneimine", Chemistry of Materials, vol. 21, no. 4, pp. 673-681, 2009.
[54] Y. Peng, W. Si, X. Li, J. Luo, J. Li, J. Crittenden and J. Hao, "Comparison of MoO3 and WO3 on arsenic poisoning V2O5/TiO2 catalyst: DRIFTS and DFT study", Applied Catalysis B: Environmental, vol. 181, pp. 692-698, 2016.
[55] M. Ferhat and A. Zaoui, "Structural and electronic properties of III-V bismuth compounds", Physical Review B, vol. 73, no. 11, 2006.